International Journal of Electrical and
Electronics Engineering Research (IJEEER)
ISSN(P): 2250-155X; ISSN(E): 2278-943X
Vol. 5, Issue 4, Aug 2015, 23-44

TRANS STELLAR
• Journal Publications • Research Consultancy

HARMONIC POWER METHOD FOR HARMONIC POLLUTION IDENTIFICATION IN DISTRIBUTION SYSTEM HAVING MULTIPLE LOADS WITH LOAD POSITION SHIFTING

S. V. D. ANIL KUMAR[1] & K. RAMESH REDDY[2]

[1]Associate Professor, Department of EEE, St. Ann's College of Engineering and Tech, Chirala, Andhra Pradesh, India

[2] HOD & Dean, Department of PG Studies, GNITS, Hyderabad, Telangana, India

ABSTRACT

In recent years, with the fast development of the facility electronic technology, numerous power electronic devices and nonlinear parts, particularly of the many types of rectifier and oppressor, square measure applied wide in facility. Harmonics have made serious adverse effects within the instrumentation of power generators and distribution system, and of their management and protection, yet because the users and therefore the communication fields. Hence it is very important to identify the harmonics for the further reduction. Due to the complexity in identification of harmonics compensation techniques suffers from inefficiency. To reduce the complexness of identification we've developed the Total Harmonic Power (THP) methodology is one of the methods planned among the literature for this purpose. This paper tries to point that the supply of harmonic pollution is downstream with relevance the nodes (i.e., the load is cause of harmonic pollution) caused due to two linear load and nonlinear load with Resistive and also studied the effectiveness of the concept with change in position of loads at corresponding nodes

KEYWORDS: Harmonics, Total Harmonic Power, Nonlinear Load, Resistive, Change in Position

INTRODUCTION

Identification of harmonic sources in a very power grid has been a difficult task for several years. The foremost common tool to resolve this downside is that the harmonic power direction-based technique [1]–[3]. During this technique, if harmonic active power flows from utility to consumer, the utility is taken into account because the dominant harmonic generator, and the other way around. sadly, [4] and [5] have evidenced that this qualitative technique is in theory unreliable. Another group of sensible ways for harmonic supply detection is to live the utility and client harmonic impedances and so calculate the harmonic sources behind the impedances. There is unit variety of variations of this technique [6]–[9]. Though this sort of technique is in theory sound, it's terribly tough to implement. The most downside is that the impedances will solely be determined with the assistance of disturbances. Such disturbances don't seem to be without delay accessible from the system or area unit costly to come up with intrusive means that. The incentive scheme is considered by many as an ideal solution to control harmonic generations from disturbing loads. Unfortunately, the scheme faces two major technical challenges. One challenge is the need to separate the harmonic contribution of a customer from that of the supply system. The other is to isolate the effect of utility impedance variation on customer's harmonic injection levels. Since the publication of [3], many research efforts have been directed to these problems [4]–[7]. However, there are still no satisfactory solutions.

The total harmonic power (THP) method [9] is a simple method that uses the sign of the THP at a specific node to decide on whether the source of harmonic pollution is upstream or downstream from this node. Despite its simplicity, this method suffers from two main drawbacks: 1) the concept of upstream and downstream cannot be applied to nonradial networks. 2) the sign of the THP depends on the phase shifts between the voltages and currents at different harmonic orders. Hence, any error in calculating these phase shifts affects the reliability of the method. Such a problem becomes serious for higher harmonic orders when the system has an inductive nature and the phase shifts approach 90 [9]. The capability of the THP method in identifying the source of harmonic pollution correctly has been questioned by some researchers. The results were not similar for some cases and, thus, the THP method was assumed to fail in these cases. However, using an index that is entirely designed for the method proposed in [6], as a basis for the comparison, seems unreasonable. Accordingly, the THP method was assumed to be unsuitable for some cases as it cannot accommodate this concept. However, this idea is questionable, because it assumes that a load that will increase the ability loss within the system as a result of the generation of harmonic powers will still be outlined as not a problematic load that is certainly not a sensible assumption.

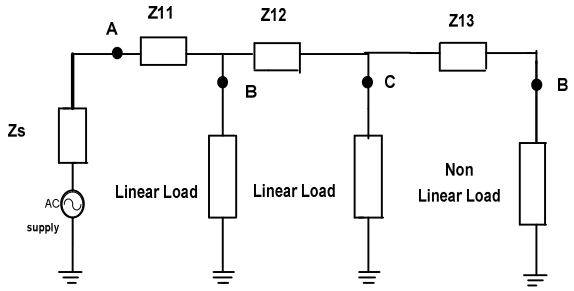

Figure 1: Simple Network with Two Linear Loads and Nonlinear Load Connected to a Sinusoidal Supply

TOTAL HARMONIC POWER METHOD

The fundamentals of the THP technique are often illustrated by using the circuit shown in Fig. 1. a perfect sinusoidal voltage source is connected to a nonlinear load through the system impedance. The nonlinear load generates harmonic currents that flow within the system inflicting voltage distortion at PCC. This voltage distortion depends on each the harmonic currents and the system electrical phenomenon at harmonic frequencies. The distorted voltage and current at PCC are often expressed by Fourier series as

$$v_{pcc}(t) = V_0 + \sum_{h=1}^{\infty} \sqrt{2} V_h \sin(h\omega_1 t + \theta_{hV}) \quad (1)$$

$$i_{pcc}(t) = V_0 + \sum_{h=1}^{\infty} \sqrt{2} I_h \sin(h\omega_1 t + \theta_{hI}) \quad (2)$$

where Vpcc(t) and ipcc(t) are the instantaneous voltage and current at point pcc, h is the harmonic order, ω_1 is the fundamental angular frequency of the supply, V_0 and I_0 are the magnitudes of dc components of the voltage and current, V_h and I_h are the rms values of the voltage and current at frequency $h\omega_1$, and θ_{hv} and θ_{hI} are the phase shifts of the *h*th harmonic voltage and current with respect to a common reference.

The instantaneous power at any point in the system is defined as

$$p(t)=v(t).i(t) \quad (3)$$

The average power at point pcc is

$$P_{pcc} = \frac{1}{T}\int_0^T pb(t)dt \quad (4)$$

$$P_{pcc}=V_0I_0 + \sum_{h=1}^{\infty} VhIh\cos\Phi h \quad (5)$$

The average power at point pcc can be decomposed into: 1) power due to dc components P_0; 2) fundamental active power P_1; and 3) total harmonic active power P_H

$$P_{pcc}=P_0+P_1+P_H \quad (6)$$

$$P_0=V_0I_0 \quad (7)$$

$$P_1=V_1I_1\cos\Phi 1 \quad (8)$$

$$P_H= \sum_{h=2}^{\infty} VhIh\cos\Phi h \quad (9)$$

Consider the voltage at point A as a reference, hence

$$v_A(t)=\sqrt{2}V_{A1}\sin(\omega 1t) \quad (10)$$

Applying the procedure outlined before to point A, the average power at A can be given by

$$P_{A1}=V_{A1}I_{B1}\cos\Phi 1 \quad (11)$$

Equation (11) demonstrates the well-known fact that a sinusoidal source delivers power only at the fundamental frequency. Some of this power is dissipated in the resistance of the system impedance and the rest flows to the load side. The nonlinear load is the only source of distortion in this case that generates harmonic currents at different frequencies. Thus, harmonic powers, with a total value of P_H flow from the load side to the supply side and are dissipated in the resistance of the system impedance [18]. As a conclusion, the nonlinear load converts power at the fundamental frequency to powers at the fundamental and harmonic frequencies. The THP method suggests that the THP at a certain node is an indication for the existence of a polluting load. Moreover, the sign of this power can be used to identify the location of the polluting load in radial systems as follows.

If P_H positive at a certain point in the system, then a harmonic source exists upstream of this point and the harmonic power is received from the source side.

If P_H is negative, then a harmonic source exists downstream of the node under study, and the harmonic power is received from the load side.

SYSTEM CONFIGURATION

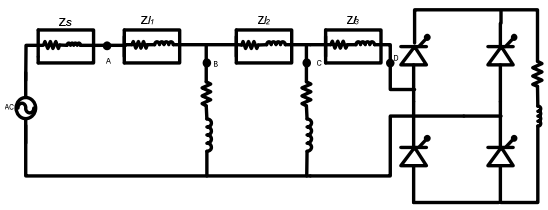

Figure 2: Linear Load at Node B, C and Nonlinear Load with RL Load at D (Load Side) Connected to a AC Supply (Condition 1)

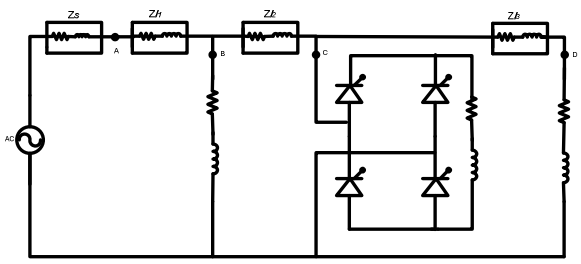

Figure 3: Linear Load at Node B, D and Nonlinear Load with RL Load at C (Middle Side) Connected to a AC Supply (Condition 2)

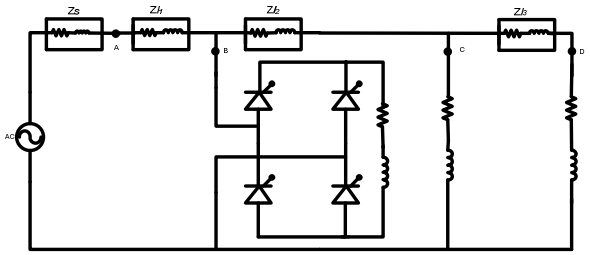

Figure 4: Linear Load at Node C, D and Nonlinear Load with RL Load at B(Source Side) Connected to a AC Supply (Condition 3)

The two linear loads and a nonlinear with RL load are connected to the supply as shown in Fig. 2. Three conditions are studied for this case: first, load 1and 2 is linear while load 2 is nonlinear (condition 1), and then, the locations of the loads are exchanged Figure 3. (Condition 2) and Figure 4. (Condition 3). The linear load is an inductive load having an impedance $Z_{L1}=2+j12.56\Omega$ at the fundamental frequency. The nonlinear load is an ac voltage regulator with two anti parallel SCRs, connected to an inductive load with impedance $Z_{L2}=2+j12.56\Omega$ and $Z_{L3}=2+j12.56\Omega$ operating at different firing angles of 30^o, 60^o, 90^o, 120^o and 150^o.

The fundamental power P1 is positive at nodes A, B, C and D decreases from the supply to the load side.

The THP P_H and each individual harmonic power are all negative at node A for both conditions. Thus, the source of harmonic pollution is downstream with respect to this node (load side).

For condition 1, the THP P_H and each individual harmonic power are all negative at node, indicating that the polluting source is downstream with respect to this node. On the other hand, these powers are positive at node, indicating that the polluting source is upstream with respect to this node. Therefore, it can be concluded that the load connected at node D (nonlinear) on load side is a harmonic polluting load.

For condition 2, the signs of the harmonic powers at nodes B and D are opposite of those obtained for condition 1 and, thus, it can be concluded that the load at node C (nonlinear) on middle side is a harmonic polluting load.

For condition 3, the signs of the harmonic powers at nodes C and D are opposite of those obtained for condition 1 and, thus, it can be concluded that the load at node B (nonlinear) on source side is a harmonic polluting load.

MATLAB/SIMULINK RESULTS

Case I: Simulation Analysis for Linear Load and Resistive Inductive based Non Linear load at $\alpha=30^0$on Load Side

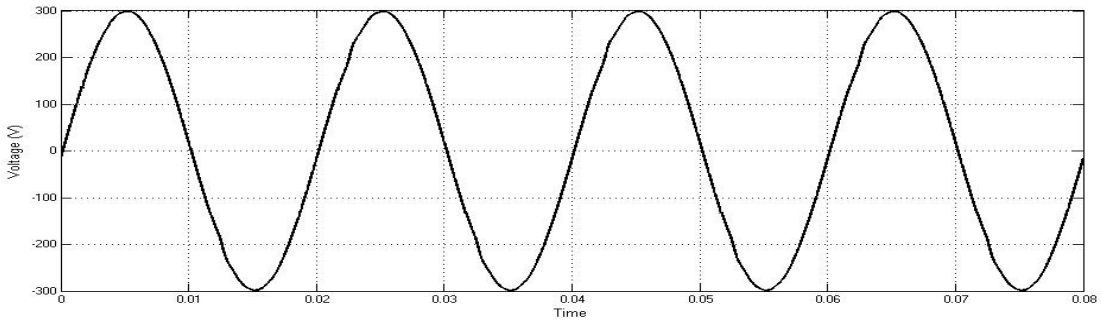

Figure 5: Simulated Voltage Wave form at Node 1 with α=30 Non-linear Load Controlled RL Load on Load Side

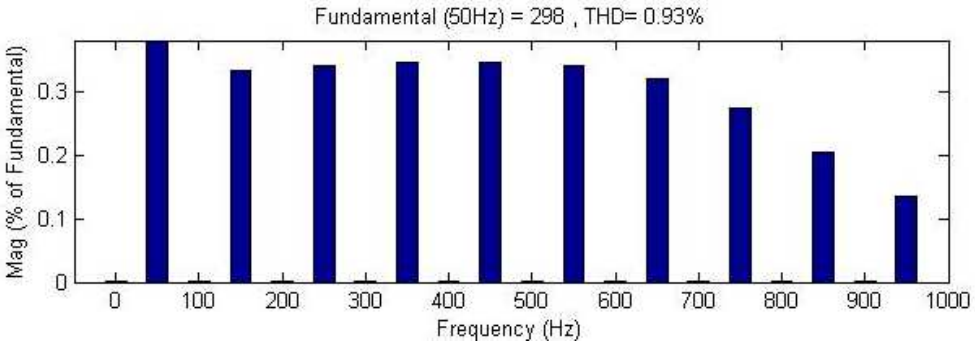

Figure 6: Total Harmonic Distortion of Voltage at Node 1 Shows 0.90% with α=30 Non-linear Load Controlled RL Load on Load Side

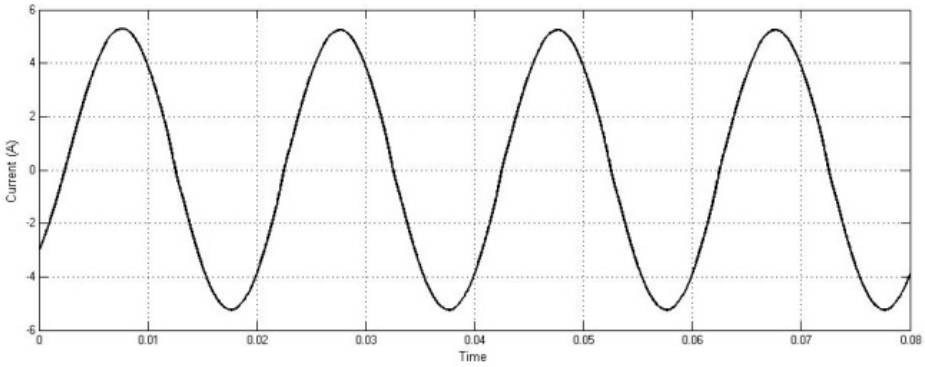

Figure 7: Simulated Current Wave form at Node 1 with α=30 Non-linear Load Controlled RL Load on Load Side

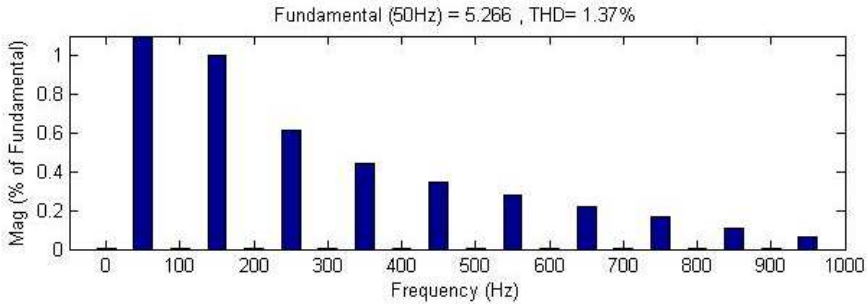

Figure 8: Total Harmonic Distortion of Current at Node 1 Shows 1.37% with α=30 Non-linear Load Controlled RL Load on Load Side

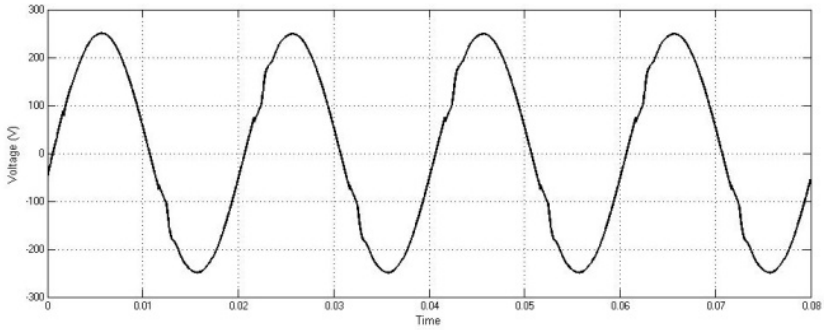

Figure 9: Simulated Voltage Wave form at Node 2 with α=30 Non-Linear Load Controlled RL Load on Load Side

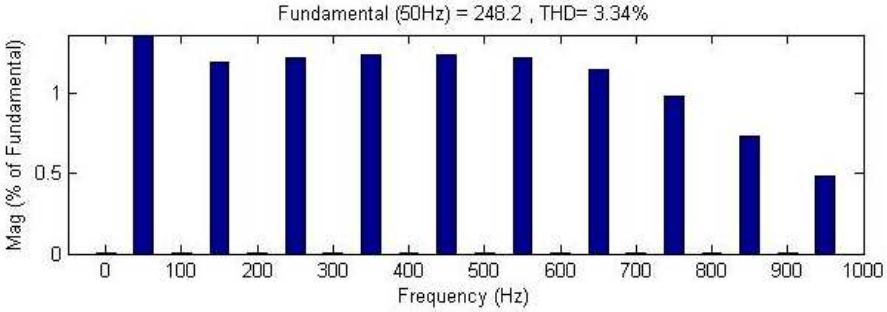

Figure 10: Total Harmonic Distortion of Voltage at Node 2 shows 3.34% with α=30 Non-Linear Load Controlled RL Load on Load Side

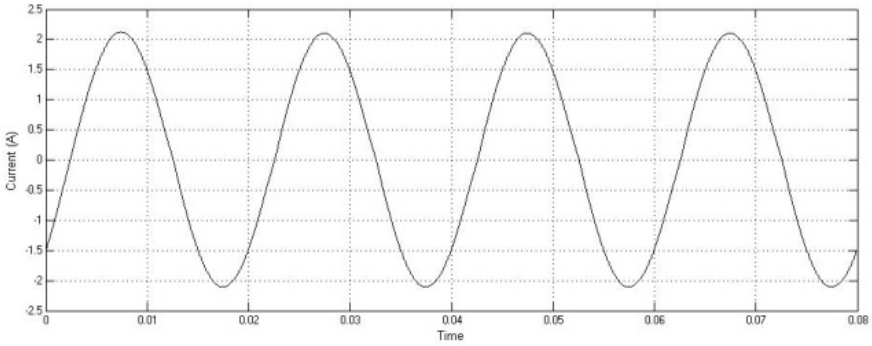

Figure 11: Simulated Current Wave form at Node 2 with α=30 Non-Linear Load Controlled RL Load on Load Side

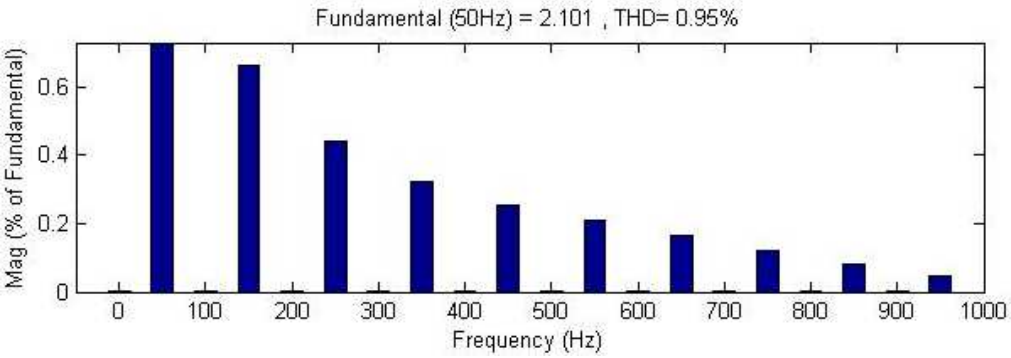

Figure 12: Total Harmonic Distortion of Current at Node 2 Shows 0.95% with α=30 Non-linear Load Controlled RL Load on Load Side

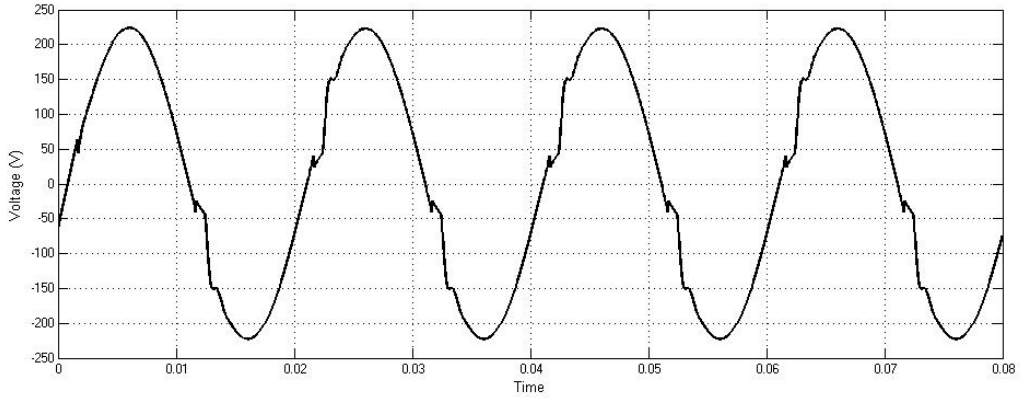

Figure 13: Simulated Voltage Wave Form at Node 3 with α=30 Non-Linear Load Controlled RL Load on Load Side

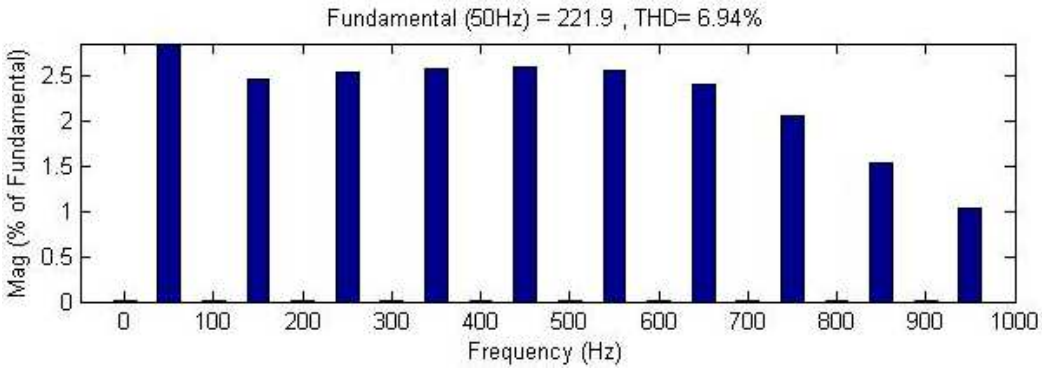

Figure 14: Total Harmonic Distortion of Voltage at Node 3 Shows 6.94% with α=30 Non-linear Load Controlled RL Load on Load Side

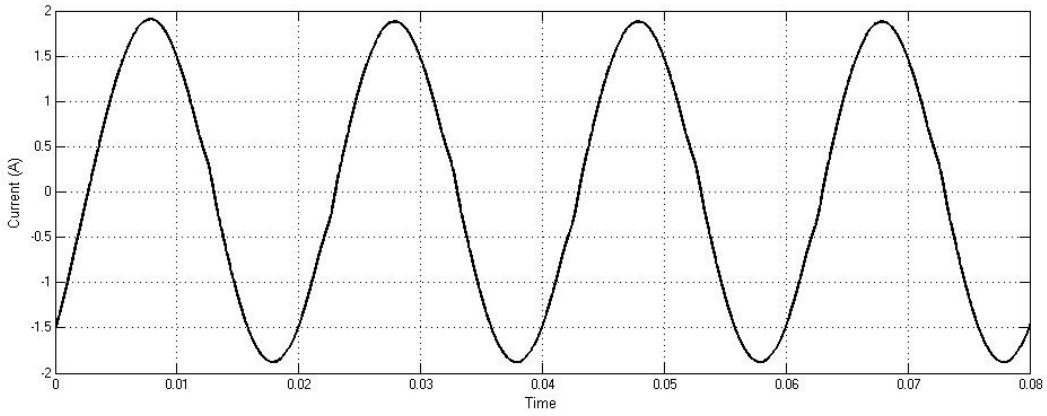

Figure 15: Simulated Current Wave form at Node 3 with α=30 Non-Linear Load Controlled RL Load on Load Side

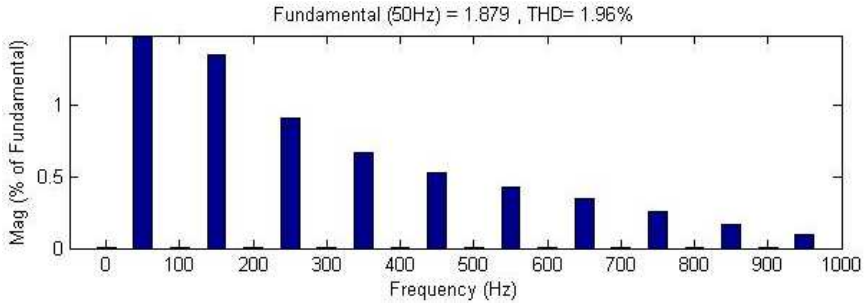

Figure 16: Total Harmonic Distortion of Current at Node 3 Shows 1.96% with α=30 Non-Linear Load Controlled RL Load on Load Side

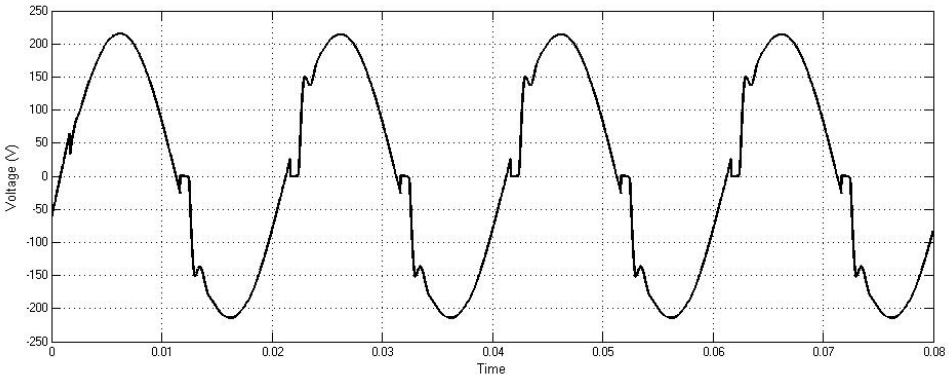

Figure 17: Simulated Voltage Wave form at Node 4 with α=30 Non-linear Load Controlled RL Load on Load Side

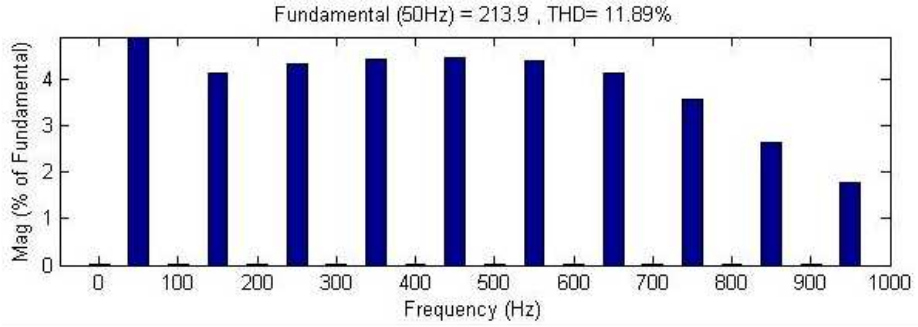

Figure 18: Total Harmonic Distortion of Voltage at Node 4 Shows 11.98% with α=30 Non-linear Load Controlled RL Load on Load Side

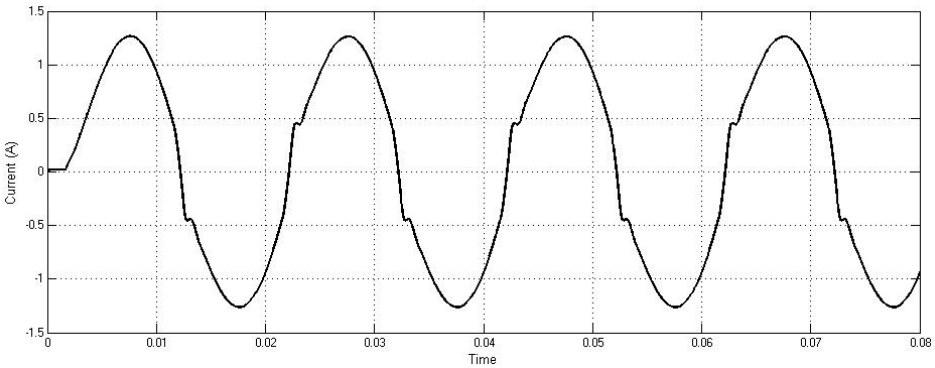

Figure 19: Simulated Current Wave form at Node 4 with α=30 Non-linear Load Controlled RL Load on Load Side

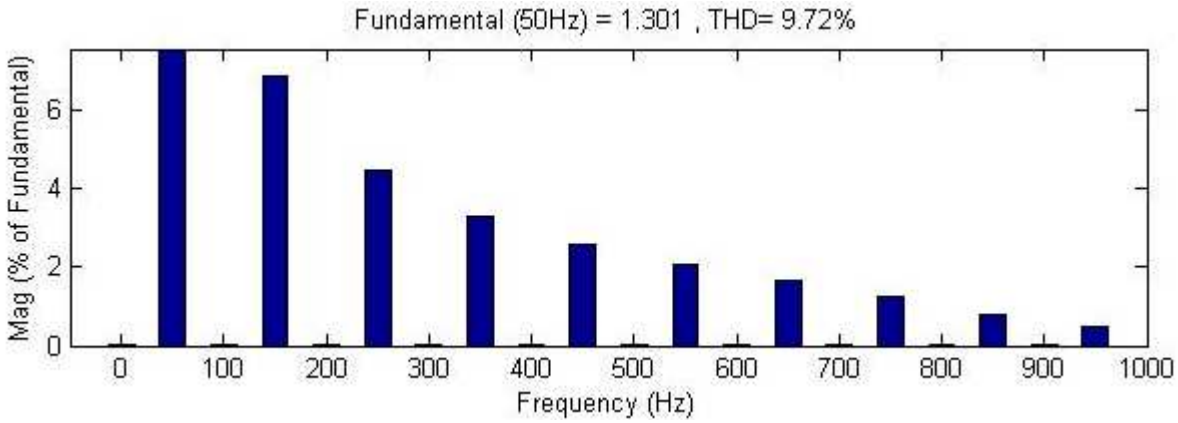

Figure 20: Total Harmonic Distortion of Current at Node 4 Shows 9.72% with α=30 Non-linear Load Controlled RL Load on Load Side

Case II: Simulation analysis for linear load and Resistive Inductive based Non linear load at α=30^{0}on middle side

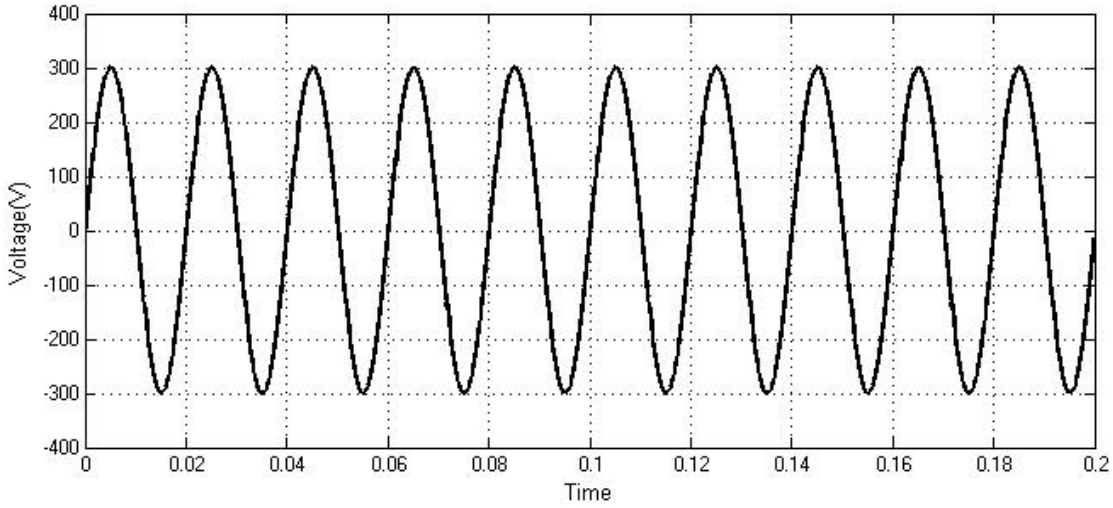

Figure 21: Simulated Voltage Wave form at Node 1 with α=30 Non-linear Load Controlled RL Load on Middle Side

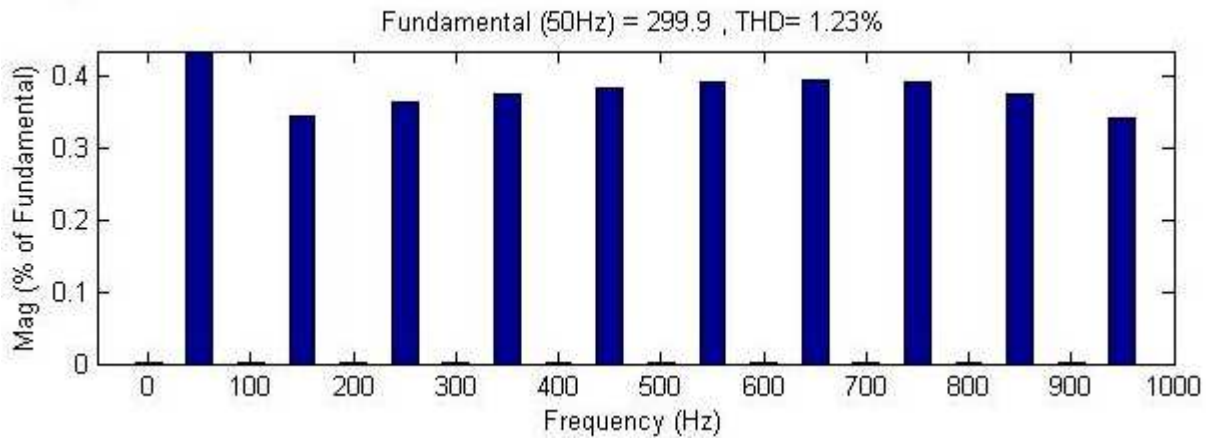

Figure 22: Total Harmonic Distortion of Voltage at Node 1 Shows 1.23% with α=30 Non-linear Load Controlled RL Load on Middle Side

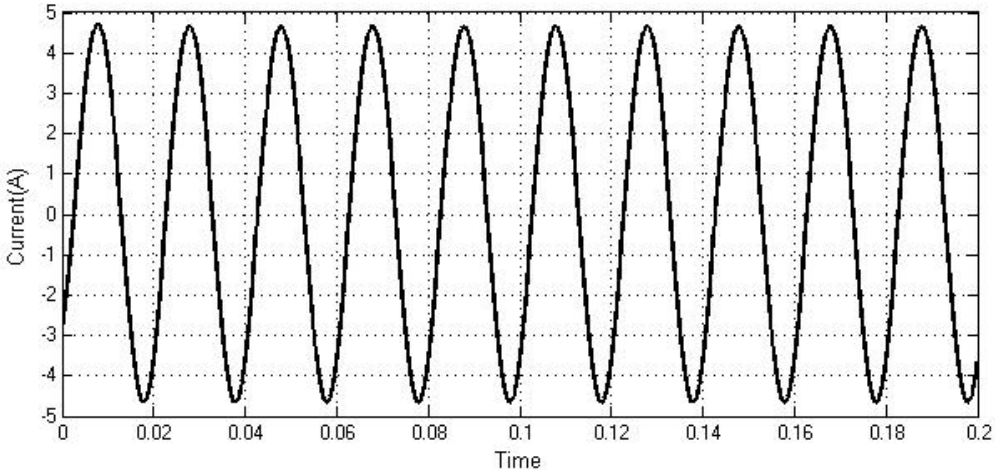

Figure 23: Simulated Current Wave form at Node 1 with α=30 Non-linear Load Controlled RL Load on Middle Side

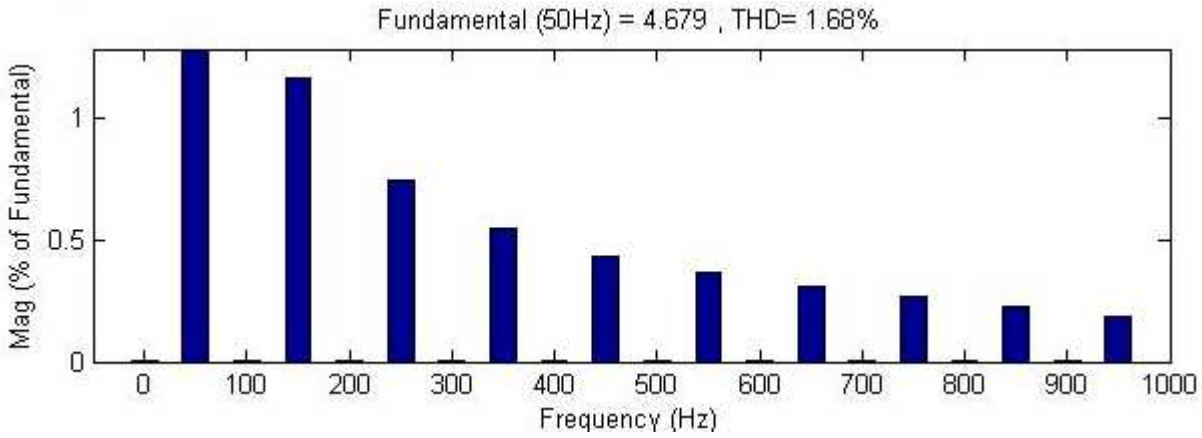

Figure 24: Total Harmonic Distortion of Current at Node 1 Shows 1.68% with α=30 Non-linear Load Controlled RL Load on Middle Side

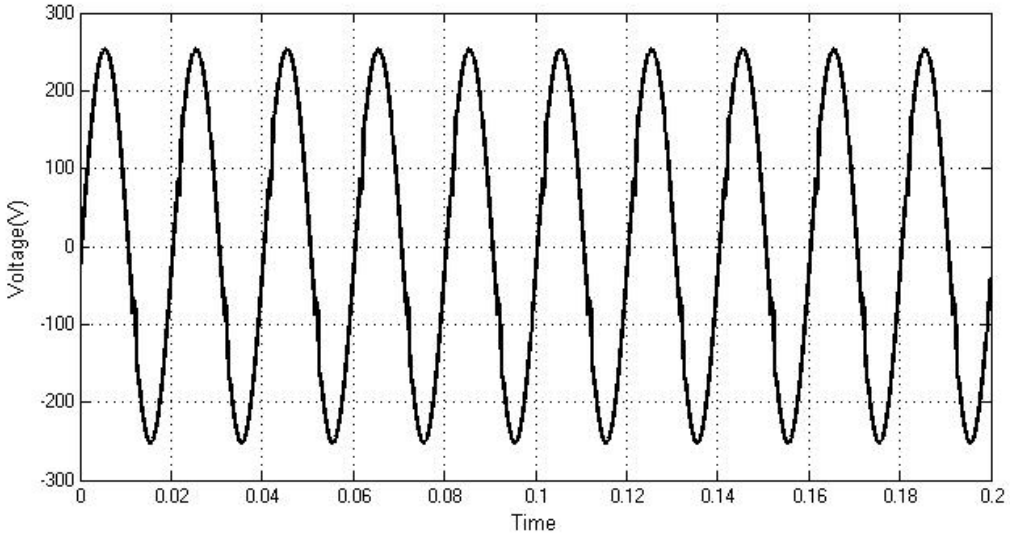

Figure 25: Simulated Voltage Wave form at Node 2 with α=30 Non-linear Load Controlled RL Load on Middle Side

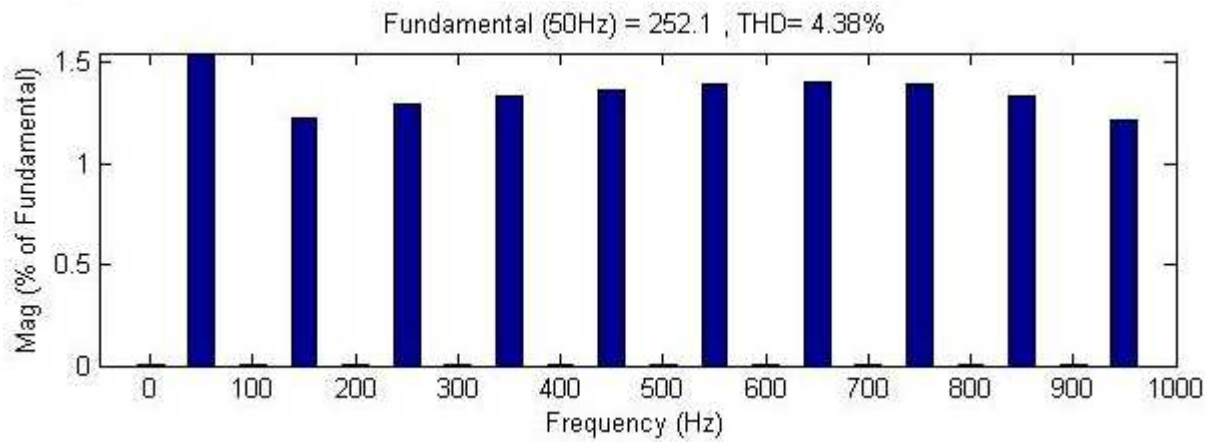

Figure 26: Total Harmonic Distortion of Voltage at Node 2 Shows 4.38% with α=30 Non-linear Load Controlled RL Load on Middle Side

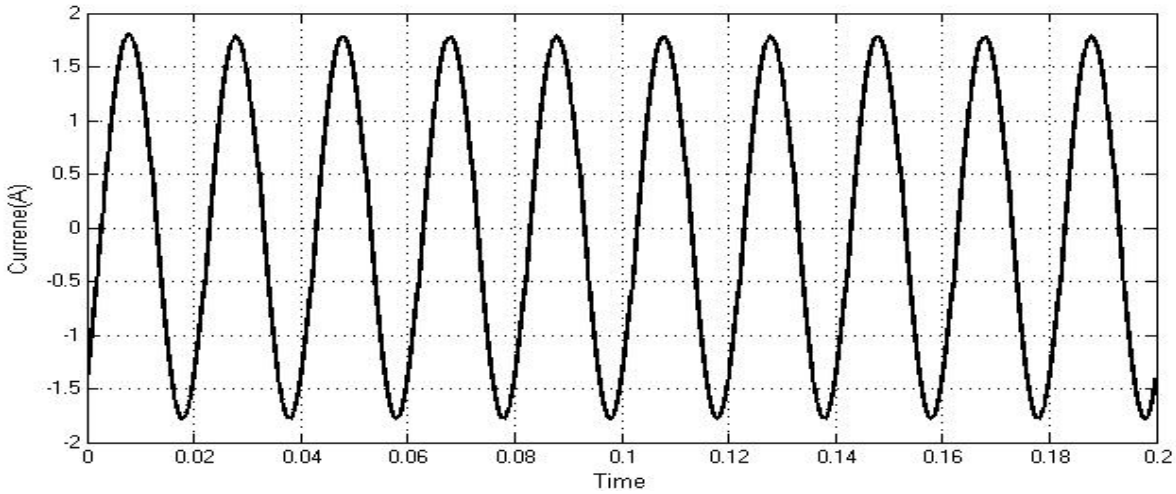

Figure 27: Simulated Current Wave form at Node 2 with α=30 Non-linear Load Controlled RL Load on Middle Side

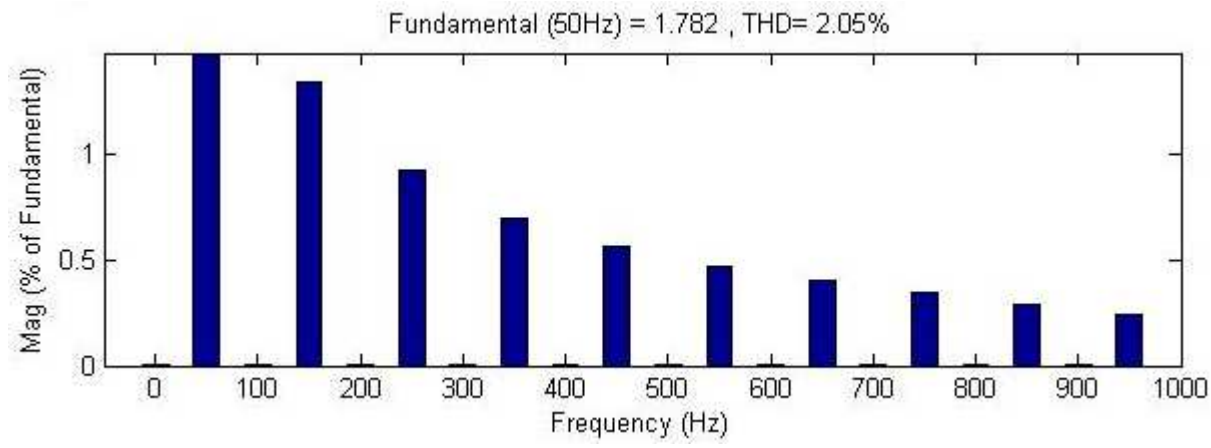

Figure 28: Total Harmonic Distortion of Current at Node 2 Shows 2.05% with α=30 Non-linear Load Controlled RL Load on Middle Side

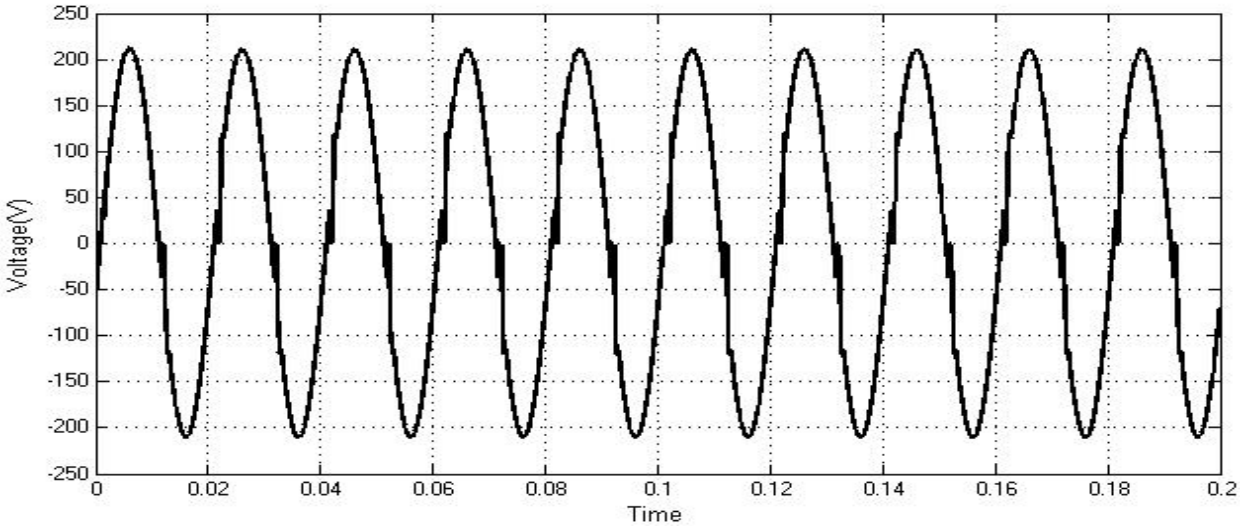

Figure 29: Simulated Voltage Wave form at Node 3 with α=30 Non-linear Load Controlled RL Load on Middle Side

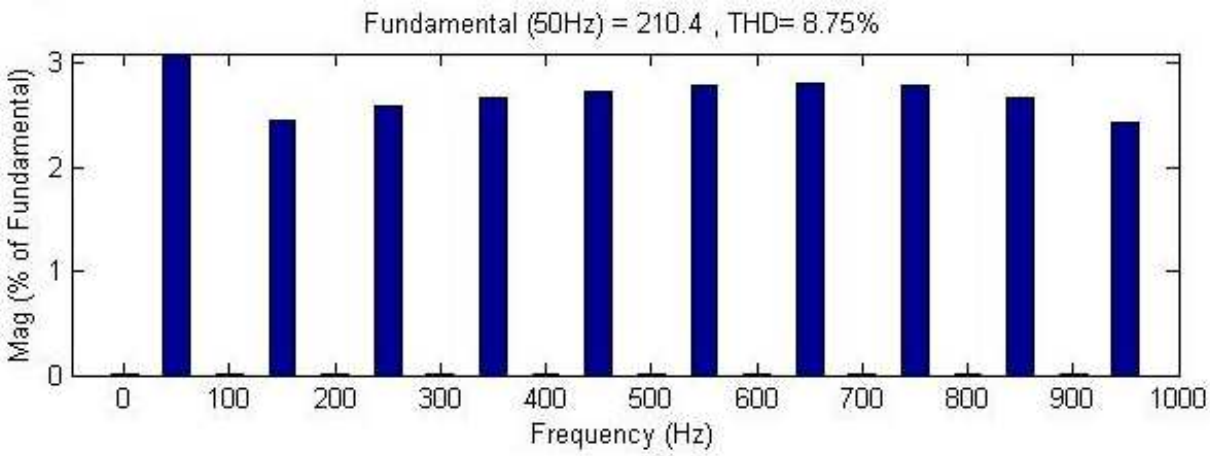

Figure 30: Total Harmonic Distortion of Voltage at Node 3 Shows 8.75% with α=30 Non-linear load Controlled RL Load on Middle Side

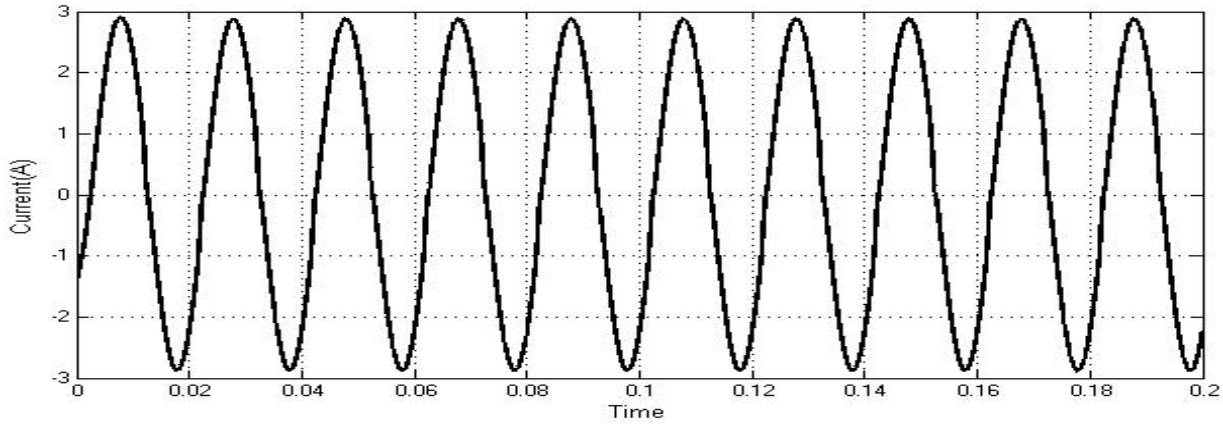

Figure 31: Simulated Current Wave form at Node 3 with α=30 Non-linear Load Controlled RL Load on Middle Side

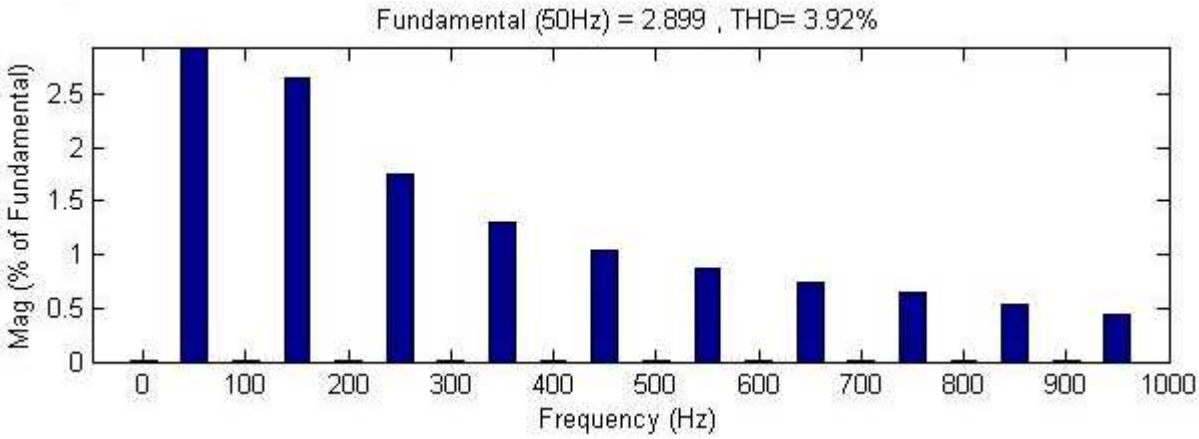

Figure 32: Total Harmonic Distortion of Current at Node 3 Shows 3.92 with α=30 Non-linear Load Controlled RL Load on Middle Side

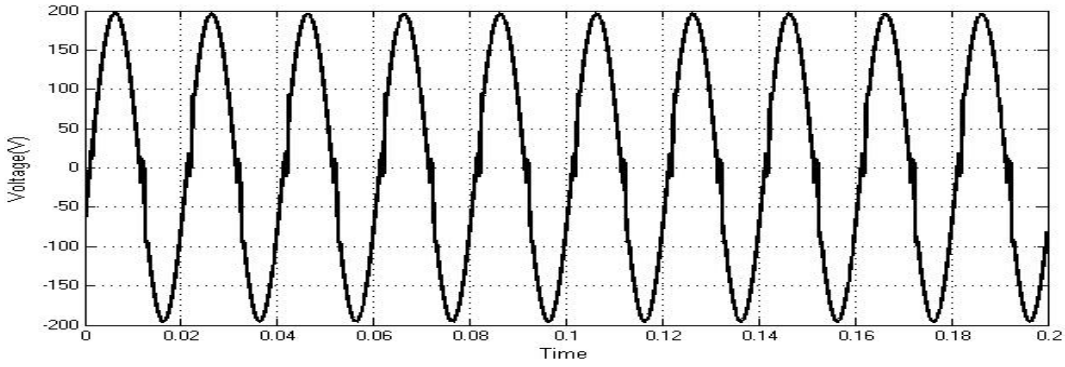

Figure 33: Simulated Voltage Wave form at Node 4 with α=30 Non-linear Load Controlled RL Load on Middle Side

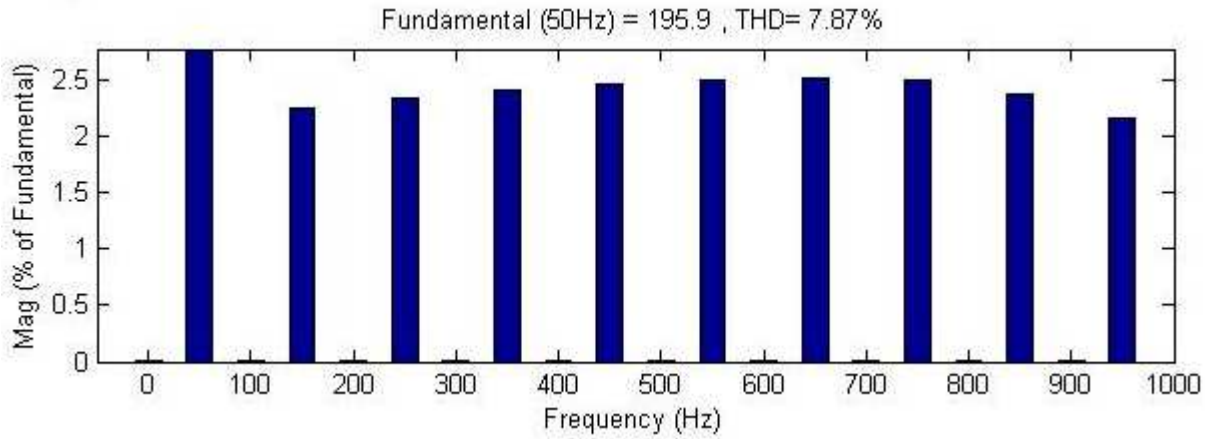

Figure 34: Total Harmonic Distortion of Voltage at Node 4 Shows 7.87% with α=30 Non-linear Load Controlled RL Load on Middle Side

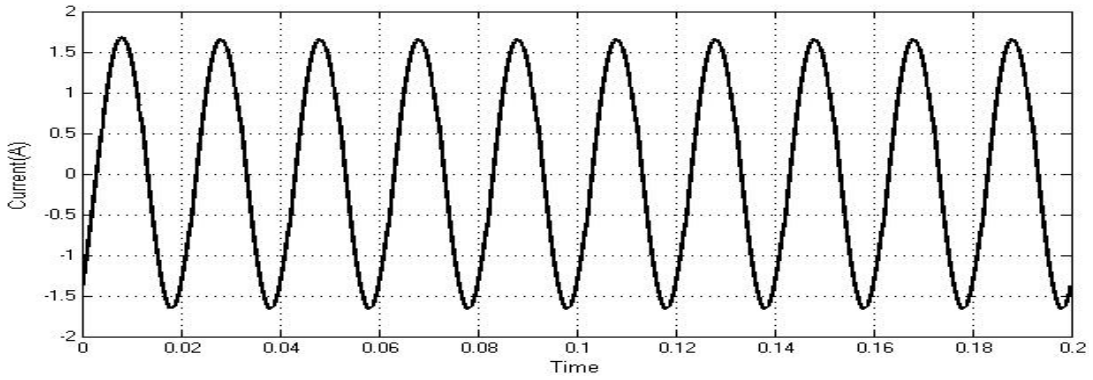

Figure 35: Simulated Current Wave form at Node 4 with α=30 Non-linear Load Controlled RL Load on Middle Side

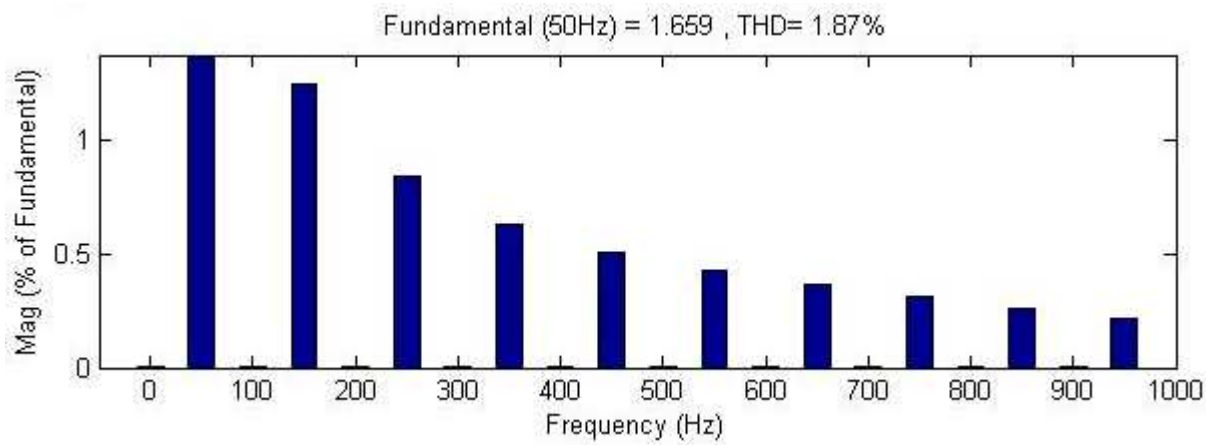

Figure 36: Total Harmonic Distortion of Current at Node 4 Shows 1.87% with α=30 Non-linear Load Controlled RL Load on Middle Side

Case III: Simulation analysis for linear load and Resistive Inductive based Non linear load at α=30^{0}on Source side

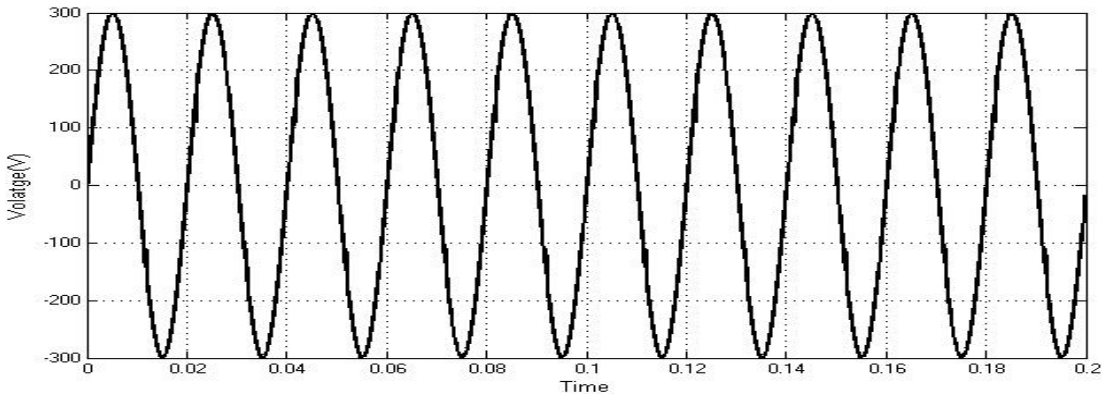

Figure 37: Simulated Voltage Wave form at Node 1 with α=30 Non-linear Load Controlled RL Load on Source Side

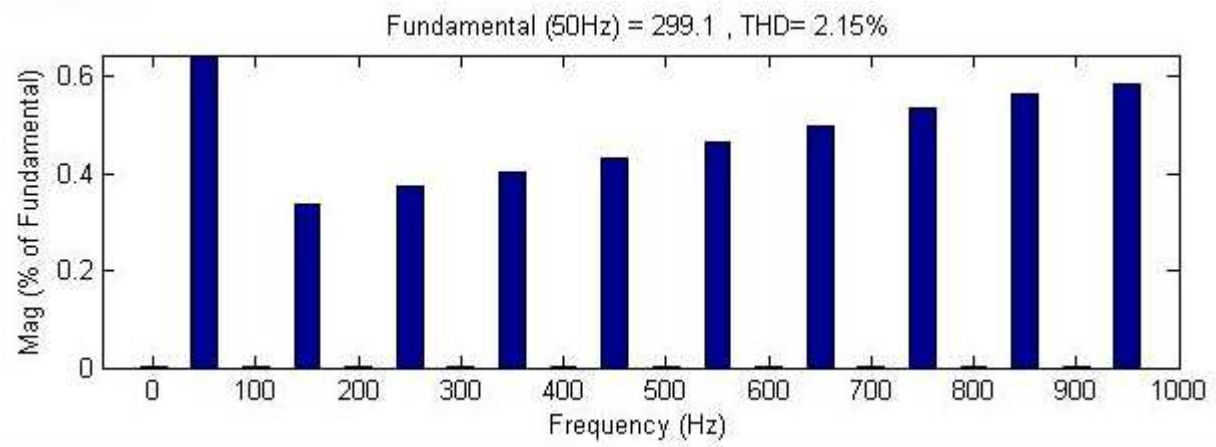

Figure 38: Total Harmonic Distortion of Voltage at Node 1 Shows 2.15% with α=30 Non-linear Load Controlled RL Load on Source Side

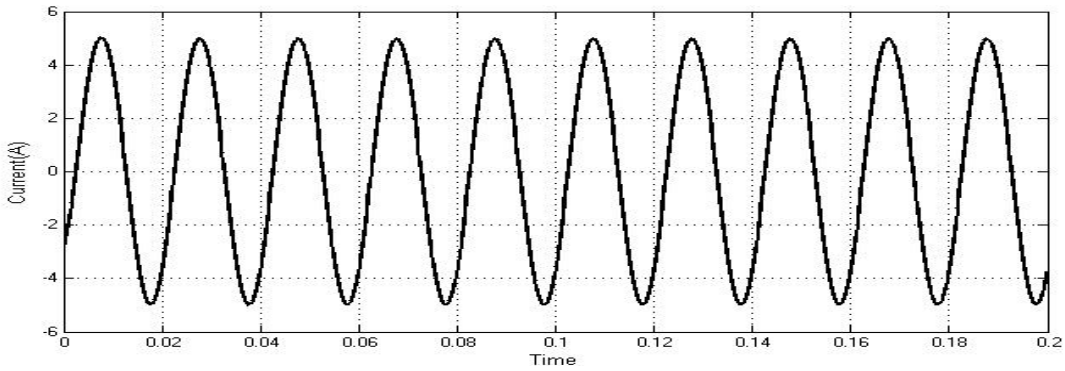

Figure 39: Simulated Current wave form at Node 1 with α=30 Non-linear Load Controlled RL Load on Source Side

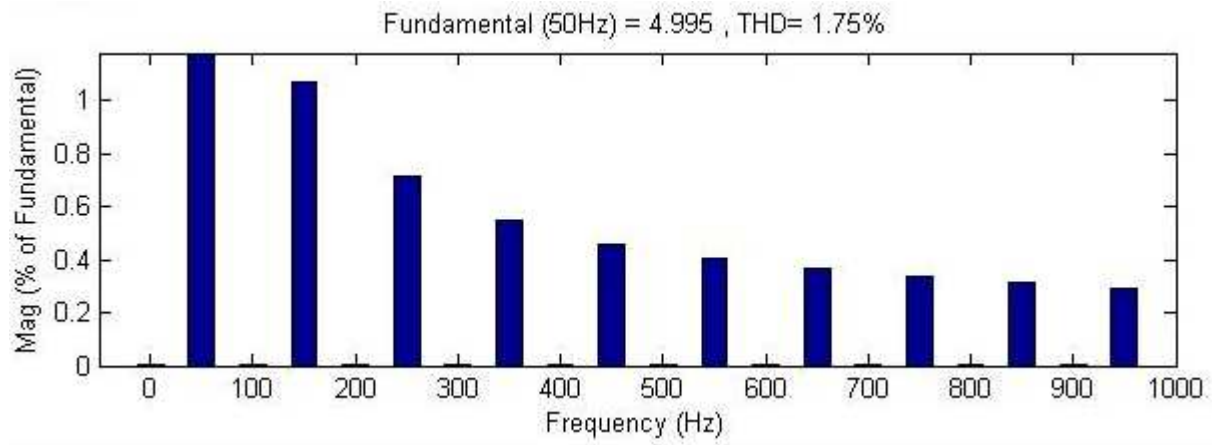

Figure 40: Total Harmonic Distortion of Current at Node 1 Shows 1.75% with α=30 Non-linear Load Controlled RL Load on Source Side

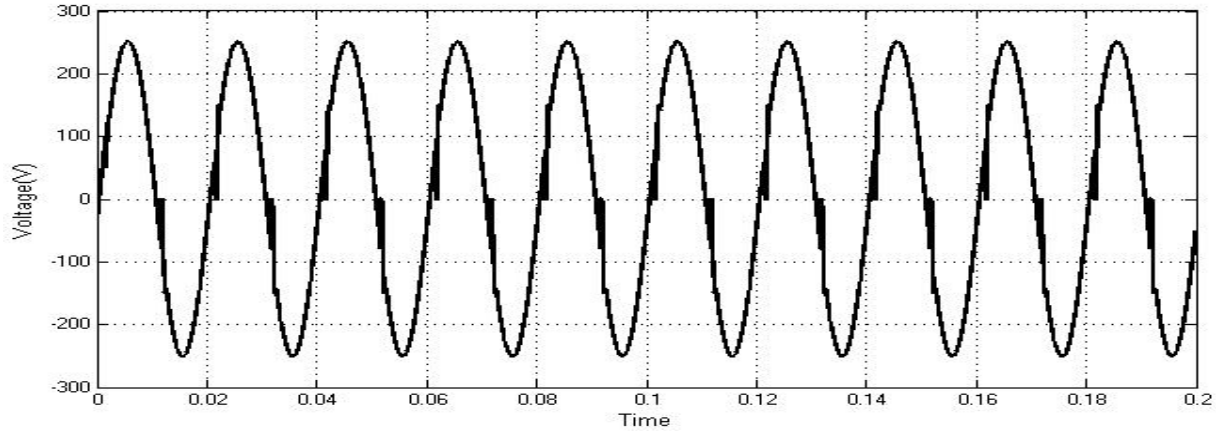

Figure 41: Simulated Voltage Wave form at Node 2 with α=30 Non-linear Load Controlled RL Load on Source Side

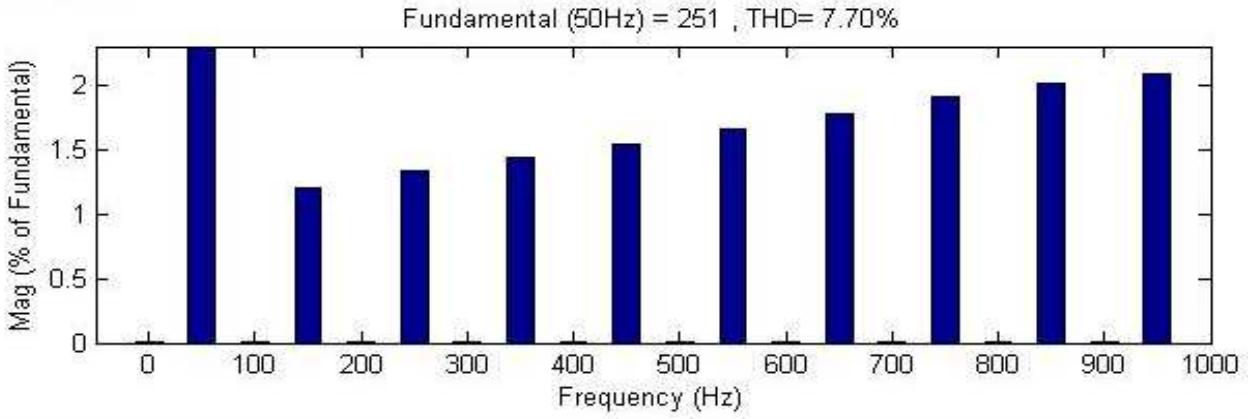

Figure 42: Total Harmonic Distortion of Voltage at Node 2 Shows 7.70% with α=30 Non-linear Load Controlled RL Load on Source Side

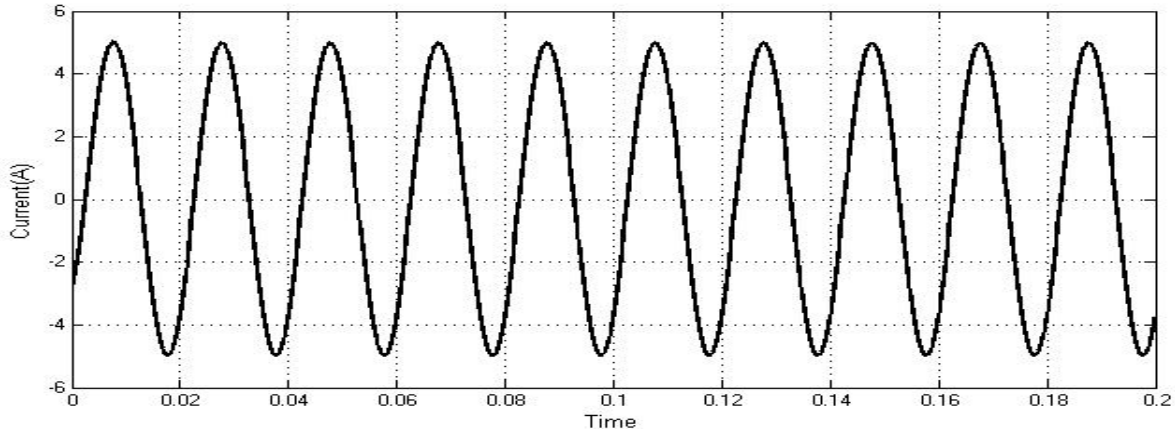

Figure 43: Simulated Current wave form at Node 2 with α=30 Non-linear Load controlled RL Load on Source Side

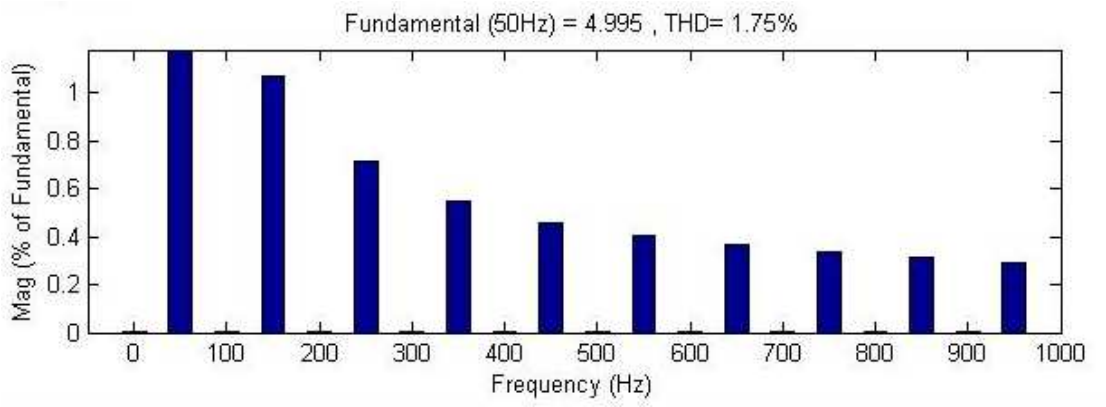

Figure 44: Total Harmonic Distortion of Current at Node 2 Shows 1.75% with α=30 Non-linear Load Controlled RL Load on Source Side

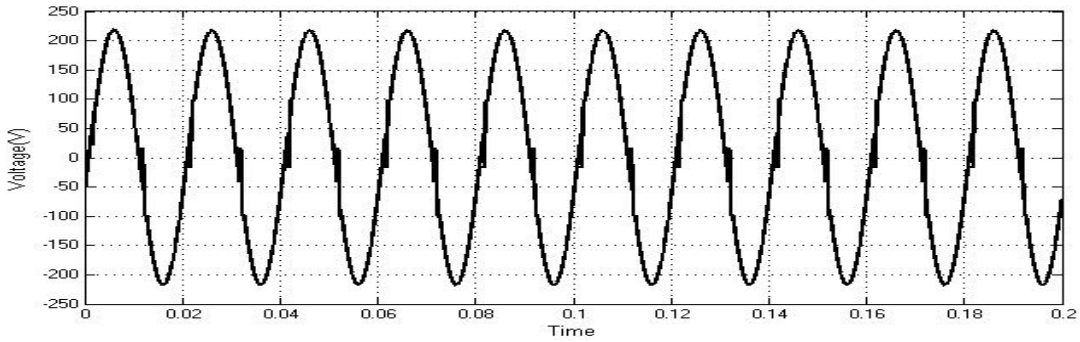

Figure 45: Simulated Voltage Wave form at Node 3 with α=30 Non-linear Load Controlled RL Load on Source Side

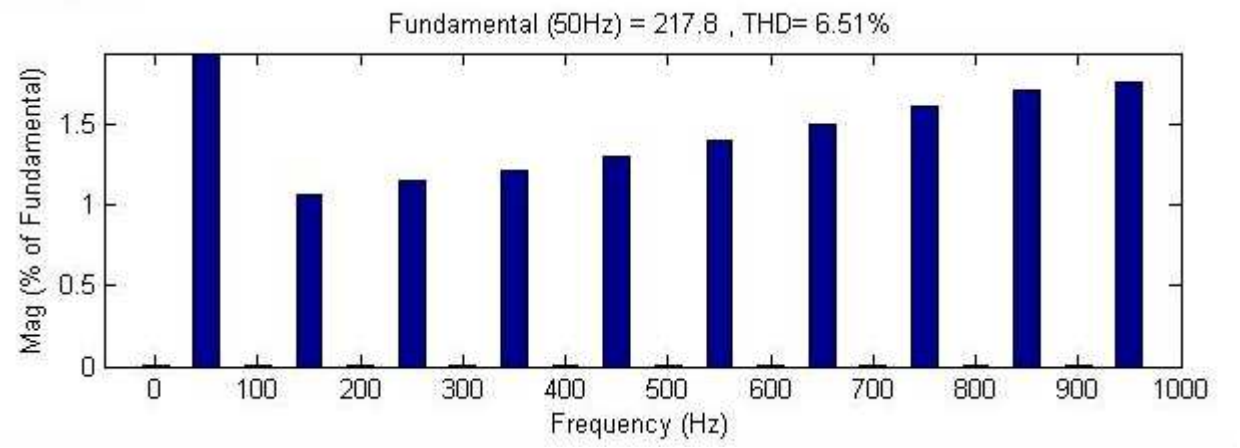

Figure 46: Total Harmonic Distortion of Voltage at Node 3 Shows 6.51% with α=30 Non-linear Load Controlled RL Load on Source Side

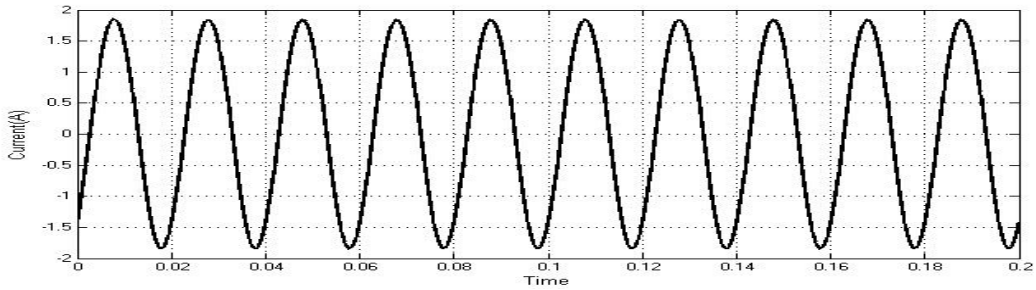

Figure 47: Simulated Current Wave form at Node 3 with α=30 Non-linear Load Controlled RL Load on Source Side

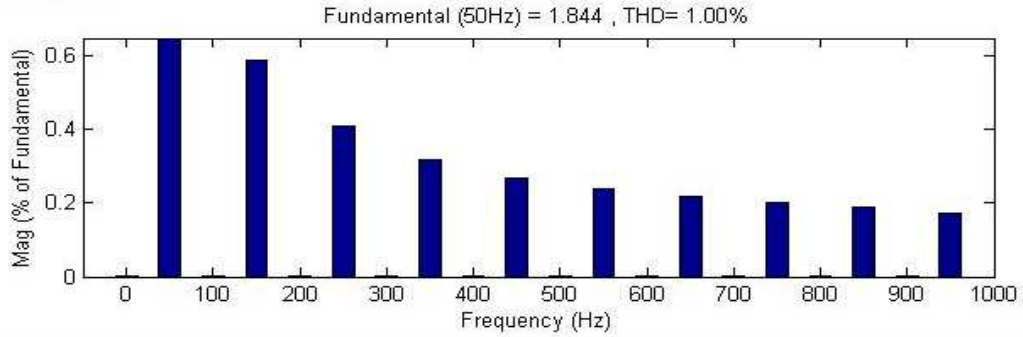

Figure 48: Total Harmonic Distortion of Current at Node 3 Shows 1 % with α=30 Non-linear Load Controlled RL Load on Source Side

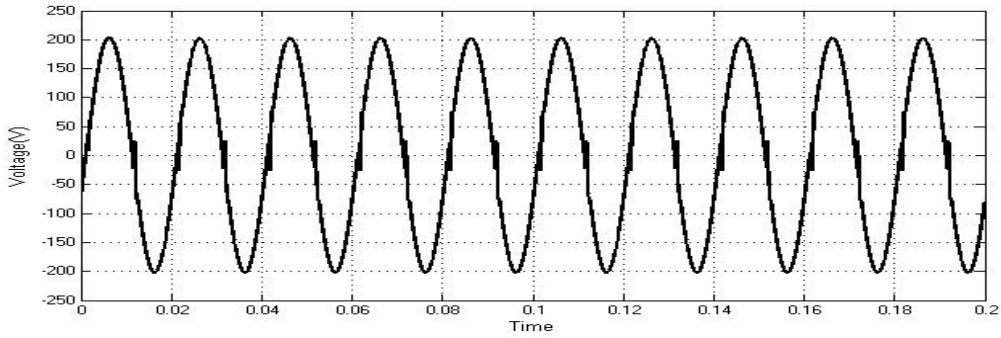

Figure 49: Simulated Voltage Wave form at Node 4 with α=30 Non-linear Load Controlled RL Load on Source Side

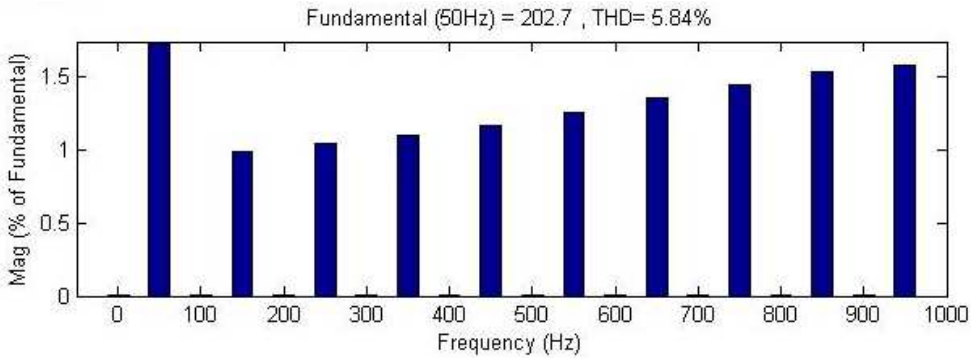

Figure 50: Total Harmonic Distortion of Voltage at Node 4 Shows 5.84% with α=30 Non-linear Load Controlled RL Load on Source Side

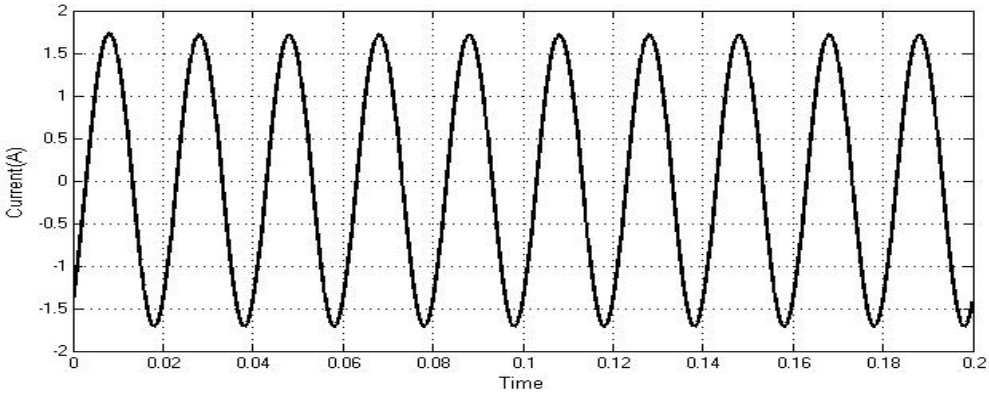

Figure 51: Simulated Current Wave form at Node 4 with α=30 Non-linear Load Controlled RL Load on Source Side

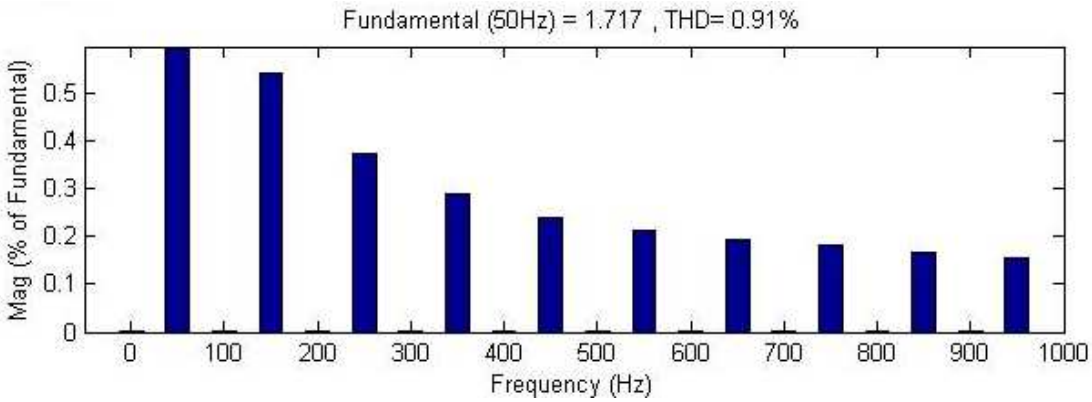

Figure 52: Total Harmonic Distortion of Current at Node 4 Shows 0.91% with α=30 Non-linear Load Controlled RL Load on Source Side

Table 1: Harmonics in Voltages and Currents with Rectifier Controlled RL-Load ON LOAD SIDE

Firing Angle	V_1	I_1	V_2	I_2	V_3	I_3	V_4	I_4
$\alpha = 30^0$	0.93	1.37	3.34	0.95	6.94	1.96	11.89	9.72
$\alpha = 60^0$	0.56	0.77	2.04	0.52	4.25	1.07	7.36	5.94
$\alpha = 90^0$	1.08	2.58	3.89	1.59	7.95	3.26	13.58	24.36
$\alpha = 120^0$	1.12	3.17	3.96	1.78	8.02	3.59	13.46	49.01
$\alpha = 150^0$	0.76	1.99	2.66	1.06	5.31	2.10	8.79	92.88

Table 2: Harmonics in Voltages and Currents with Rectifier Controlled RL-Load ON MIDDLE SIDE

Firing Angle	V_1	I_1	V_2	I_2	V_3	I_3	V_4	I_4
$\alpha = 30^0$	**1.23**	**1.68**	**4.38**	**2.05**	**8.75**	**3.92**	**7.87**	**1.87**
$\alpha = 60^0$	**0.65**	**0.96**	**2.33**	**1.14**	**4.68**	**2.27**	**4.21**	**1.04**
$\alpha = 90^0$	**1.20**	**2.89**	**4.26**	**3.13**	**8.51**	**7.00**	**7.72**	**2.88**
$\alpha = 120^0$	**1.24**	**3.51**	**4.36**	**3.40**	**8.57**	**9.12**	**7.80**	**3.13**
$\alpha = 150^0$	**0.87**	**2.23**	**3.01**	**2.01**	**5.82**	**6.34**	**5.27**	**1.84**

Table 3: Harmonics in Voltages and Currents with Rectifier Controlled RL-Load ON SOURCE SIDE

Firing Angle	V_1	I_1	V_2	I_2	V_3	I_3	V_4	I_4
$\alpha = 30^0$	**2.15**	**1.75**	**7.70**	**1.75**	**6.51**	**1.0**	**5.84**	**0.91**
$\alpha = 60^0$	**1.58**	**2.21**	**5.65**	**2.21**	**4.81**	**1.21**	**4.33**	**1.10**
$\alpha = 90^0$	**2.14**	**4.78**	**7.64**	**4.78**	**6.56**	**2.37**	**5.95**	**2.19**
$\alpha = 120^0$	**2.00**	**5.07**	**7.01**	**5.07**	**6.03**	**2.24**	**5.47**	**2.07**
$\alpha = 150^0$	**1.24**	**2.66**	**4.29**	**2.66**	**3.66**	**1.09**	**3.30**	**1.00**

Table 4: Harmonic Power with Rectifier Controlled RL-Load ON LOAD SIDE

Power (W)	$\alpha = 30^0$				$\alpha = 60^0$				$\alpha = 90^0$				$\alpha = 120^0$				$\alpha = 150^0$			
P1	569.2	220.8	176.5	132.5	538.5	220.5	175	105.8	505.5	225	180	67.14	483.1	235	194	27.06	481.7	244.3	208.5	4.921
P3	-0.00139	0.0097	0.03252	-0.05	-0.03	0.002	0.009	-0.01	-0.09	0.04	0.16	-0.32	-0.010	0.07	0.238	-0.435	-0.002	0.021	0.071	-0.12
P5	-0.00053	0.0042	0,01468	-0.02	-0.07	0.001	0.004	-0.05	-0.02	0.01	0.03	-0.074	-0.001	0.005	0.001	-0.003	-0.002	0.004	0.016	-0.024
P7	-0.00028	0.0023	0.00810	-0.01	-0.08	0.005	0.001	-0.02	-0.04	0.01	0.04	-0.010	-0.003	0.002	0.007	-0.013	0.0003	0.004	0.001	0.003

Power (W)	$\alpha = 30^0$				$\alpha = 60^0$				$\alpha = 90^0$				$\alpha = 120^0$				$\alpha = 150^0$			
P1	569.2	220.8	176.5	132.5	538.5	220.5	175	105.8	505.5	225	180	67.14	483.1	235	194	27.06	481.7	244.3	208.5	4.921
P3	-0.00139	0.0097	0.03252	-0.05	-0.03	0.002	0.009	-0.01	-0.09	0.04	0.16	-0.32	-0.010	0.07	0.238	-0.435	-0.002	0.021	0.071	-0.12
P5	-0.00053	0.0042	0,01468	-0.02	-0.07	0.001	0.004	-0.05	-0.02	0.01	0.03	-0.074	-0.001	0.005	0.001	-0.003	-0.002	0.004	0.016	-0.024
P7	-0.00028	0.0023	0.00810	-0.01	-0.08	0.005	0.001	-0.02	-0.04	0.01	0.04	-0.010	-0.003	0.002	0.007	-0.013	0.0003	0.004	0.001	0.003

Table 5: Harmonic Power with Rectifier Controlled RL-Load ON MIDDLE SIDE

Power (W)	$\alpha = 30^0$				$\alpha = 60^0$				$\alpha = 90^0$				$\alpha = 120^0$				$\alpha = 150^0$			
P1	470.9	165	268.3	137.6	440.2	166.1	241.6	136	408	173	209	140.2	385.9	184.6	180.4	149.8	383.4	195.3	168.7	160.3
P3	-0.0014	0.0172	-0.0361	0.021	-0.02	0.006	-0.011	0.007	-0.01	0.08	-0.2	0.1044	-0.010	0.114	-0.24	0.1407	-0.002	0.034	-0.071	0.042
P5	-0.000606	0.0081	-0.0166	0.009	0.006	0.002	-0.003	0.002	-0.00	0.01	-0.0421 4	0.0194	-0.001	0.001	-0.02	0.0012	0.0003	0.007	-0.012	0.009
P7	-0.000341	0.0046	-0.0095	0.005	0.007	0.009	-0.001	0.001	-0.04	0.01	-0.4	0.0018	-0.003	0.003	-0.07	0.003	0.008	0.003	0.003	0.003

Table 6: Harmonic Power with Rectifier Controlled RL-Load ON SOURCE SIDE

Power (W)	$\alpha = 30^0$				$\alpha = 60^0$				$\alpha = 90^0$				$\alpha = 120^0$				$\alpha = 150^0$			
P1	533.	508.9	170	147.3	490.4	466.8	168.7	146.2	437.5	417	172	149.5	398.7	381.7	180.4	156.4	387.7	372.6	188.3	163.2
P3	-0.001277	-0.003	0.00578	0.004	-0.06	-0.002	0.013	0.009	-0.04	-0.11	0.09	0.0689	-0.022	-0.06	0.085	0.0632	-0.003	-0.01	0.01	0.011
P5	-0.00058	-0.001	0.00282	0.002	0.007	0.002	0.004	0.003	-0.06	-0.2	0.01	0.008	-0.007	-0.02	0.001	0.013	0.009	-0.02	0.005	0.003
P7	-0.00036	-0.001	0.00171	0.001	0.008	0.002	0.001	0.001	-0.06	-0.1	0.03	0.002	-0.00	-0.02	0.002	0.018	0.004	0.001	0.00	0.003

CONCLUSIONS

In this paper it has been studied the recognition of harmonic pollution caused due to Non linear load controlled resistive inductive load. The harmonic analysis has done with non linear load controlled with $\alpha=30^0$, 60^0, 90^0, 120^0 and 150^0. (Condition 1), then, the locations of the loads are exchanged to middle side (condition 2) and finally the harmonics are tested with non linear load at source side(condition 3). Due to page limitations only wave forms at 30^0 has been shown and remaining analysis at 60^0, 90^0, 120^0 and 150^0 is shown in tabular forms for both without and with change in the loads position at corresponding nodes. The harmonic caused due these non radial loads has been efficiently recognized and calculated with Total Harmonic Power method. From the simulation analysis it is proved that for a certain node in the system, the sign of the fundamental power can be used as a reference, while the signs of the harmonic powers are compared to this reference sign to specify the responsibility of the load connected to this node to the harmonic pollution. The new modification was applied to several case studies and proved to be successful.

REFERENCES

1. W. M. Grady and S. Santoso, "Understanding power system harmonics," *IEEE Power Eng. Rev.*, vol. 21, no. 11, p. c2, Nov. 2001.
2. L. F. Beites, J. G. Mayordomo, A. Hernández, and R. Asensi, "Harmonics, interharmonics and unbalances of arc furnaces: A new frequency domain approach," *IEEE Trans. Power Del.*, vol. 16, no. 4, pp. 661–668, Oct. 2001.
3. J. Arrillaga, D. A. Bradely, and P. S. Bodger, *Power System Harmonics*. New York: Wiley, 1985.
4. L. Cristaldi, A. Ferrero, and S. Salicone, "A distributed system for electric power quality measurement," in *Proc. 18th IEEE Instrumentation and Measurement Technology Conf.*, Budapest, Hungary, 2001, vol. 3, pp. 2130–2135.
5. M. Aiello, A. Cataliotti, V. Cosentino, and S. Nuccio, "A self-synchronizing instrument for harmonic source detection in power systems," *IEEE Trans. Instrum. Meas.*, vol. 54, no. 1, pp. 15–23, Feb. 2005.
6. W. Xu and Y. Liu, "A method for determining customer and utility harmonic contributions at the point of common coupling," *IEEE Trans. Power Del.*, vol. 15, no. 2, pp. 804–811, Apr. 2000.
7. C. Chen, X. Liu, D. Koval, W. Xu, and T. Tayjasanant, "Critical impedance method—A new detecting harmonic sources method in distribution systems," *IEEE Trans. Power Del.*, vol. 19, no. 1, pp. 288–297, Jan. 2004.
8. N. Hamzah, A. Mohamed, and A. Hussain, "Harmonic source location at the point of common coupling based on voltage magnitude," in *Proc. IEEE Region 10 Conf.*, Nov. 2004, vol. C, pp. 21–24.